Molecular Therapy
Oncolytics
Original Article

CAFs/tumor cells co-targeting DNA vaccine in combination with low-dose gemcitabine for the treatment of Panc02 murine pancreatic cancer

Fei Geng,[1,3] Ling Dong,[1,3] Xin Bao,[1] Qianqian Guo,[1] Jie Guo,[1] Yi Zhou,[1] Bin Yu,[1] Hui Wu,[1] Jiaxin Wu,[1] Haihong Zhang,[1] Xianghui Yu,[1,2] and Wei Kong[1,2]

[1]National Engineering Laboratory for AIDS Vaccine, School of Life Science, Jilin University, No. 2699, Street Qianjin, Changchun 130012, P.R. China; [2]Key Laboratory for Molecular Enzymology and Engineering, the Ministry of Education, School of Life Sciences, Jilin University, Changchun 130012, P.R. China

In this study, we investigate the synergistic effect of gemcitabine (Gem) and a novel DNA vaccine in the treatment of pancreatic cancer in mice and explore the anti-tumor mechanism of this combination therapy. Fibroblast activation protein α-expressing cancer-associated fibroblasts (FAPα$^+$ CAFs), a dominant component of the tumor microenvironment (TME), have been shown to modulate the extracellular matrix (ECM) to promote the growth, invasion, and metastasis of pancreatic cancer (PC). Therefore, FAPα$^+$ CAFs may be an ideal target for the treatment of PC. However, treatments that solely target FAPα$^+$ CAFs do not directly affect tumor cells. We recently constructed a novel chimeric DNA vaccine (OsFS) against human FAPα and survivin, which simultaneously targets FAPα$^+$ CAFs and tumor cells. In Panc02 tumor-bearing mice, OsFS vaccination not only reduced the proportion of immunosuppressive cells but also promoted the recruitment of tumor-infiltrating lymphocytes, which remodeled the TME to support anti-tumor immune responses. Furthermore, after depletion of regulatory T cells (Tregs) by metronomic low-dose Gem therapy, the anti-tumor effects of OsFS were enhanced. Taken together, our results indicate that the combination of the FAPα/survivin co-targeting DNA vaccine and low-dose Gem may be an effective therapy for PC.

INTRODUCTION

Pancreatic cancer (PC) is an extremely lethal malignant tumor. In recent years, the incidence and death rates of PC continued to increase, and PC is now the 4th leading cause of cancer-related death in the USA.[1] Because of the lack of efficient diagnostic and therapeutic modalities, the 5-year relative survival rate of PC is only 9%, the lowest of all cancers.[2,3]

In addition to providing nutrients for tumor growth and invasion, the tumor microenvironment (TME) also hinders anti-tumor immune responses by recruiting immunosuppressive cells such as myeloid-derived suppressor cells (MDSCs), tumor-associated macrophages (TAMs), and regulatory T cells (Tregs).[4] Stromal elements, consisting of extracellular matrix (ECM), endothelial cells, immune cells, and cancer-associated fibroblasts (CAFs), are essential constituents of the PC microenvironment and account for up to 50%–80% of the whole tumor.[4,5] Moreover, the dense desmoplastic stroma of PC contributes to chemo-and radiotherapeutic resistance.[6,7] CAFs, a dominant component of the tumor stroma, are classically known to stimulate tumor growth, suppress the anti-tumor immune response, and enhance cancer metastasis via the release of soluble factors (e.g., CXCL2) and ECM components (e.g., COL1A1).[8–12] However, CAFs are a heterogeneous population. Different phenotypes of CAFs have distinct functions.[13–15] Recent studies have shown that the removal of CAFs from PC can promote cancer progression in mouse models.[16,17] This suggests caution in the use of CAF-targeted therapies for PC and that targeting of the appropriate CAF subset is essential. Interestingly, a subset of CAFs with surface expression of fibroblast activation protein α (FAPα) has been found to support tumor growth.[18,19] Notably, FAPα is highly expressed in PC specimens, and its expression is associated with poor prognosis. Our previous study has demonstrated that a DNA vaccine targeting FAPα can significantly reduce the proportion of intratumoral FAPα$^+$ CAFs, overcome the immune suppression in the TME, and prolong the survival of mice.[20]

Recently, we have constructed a vaccine that co-targets FAPα and survivin, termed OsFS, containing human FAPα (27–760 aa) and survivin (9–142 aa) and a CpG oligonucleotide as an adjuvant motif. When combined with doxorubicin, this vaccine showed excellent anti-4T1 tumor activity.[21] Survivin is a member of the inhibitor of apoptosis protein (IAP) family that promotes PC invasion. Its high

Received 25 January 2022; accepted 22 July 2022;
https://doi.org/10.1016/j.omto.2022.07.008.

[3]These authors contributed equally

Correspondence: Hai-Hong Zhang, PhD, National Engineering Laboratory for AIDS Vaccine, School of Life Science, Jilin University, No. 2699, Street Qianjin, Changchun 130012, P.R. China.
E-mail: zhanghh@jlu.edu.cn
Correspondence: Xianghui Yu, PhD, National Engineering Laboratory for AIDS Vaccine, School of Life Science, Jilin University, No. 2699, Street Qianjin, Changchun 130012, P.R. China.
E-mail: xianghui@jlu.edu.cn

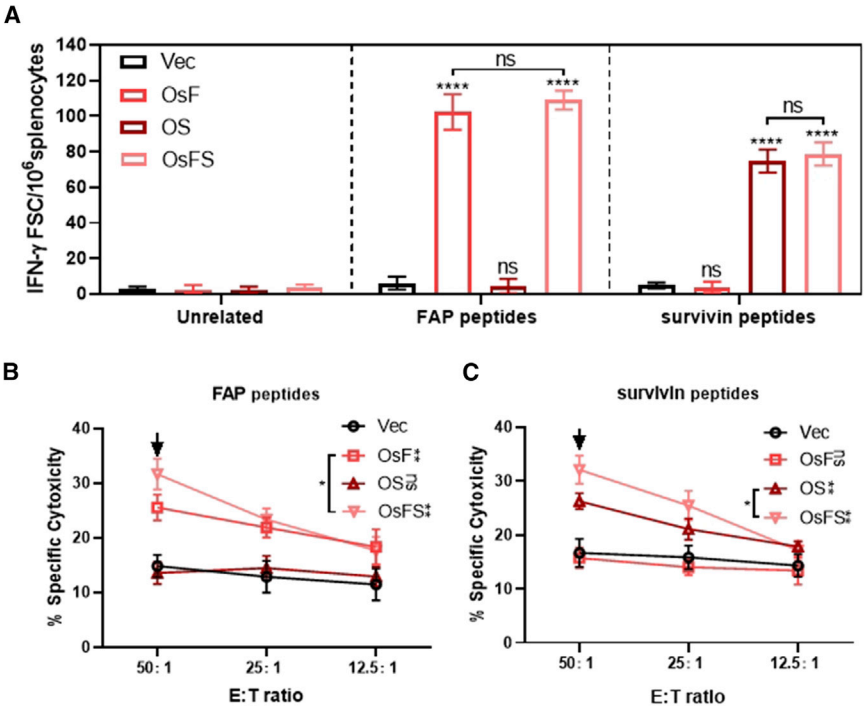

Figure 1. Analysis of immunogenicity of OsFS in C57BL/6 mice

(A) Splenocytes of vaccinated mice were stimulated with mixed FAPα, mixed survivin peptides, or unrelated peptides (human MUC1), and frequencies of antigen-specific IFN-γ-secreting T cells were measured by ELISpot. (B and C) In the CTL assay, splenocytes, as effector cells, were incubated with Panc02 cells pulsed with mouse FAPα (B) or survivin (C) peptides at different effector:target (E:T) cell ratios. Statistical significance of differences between groups was determined by unpaired Student's t test. Error bars represent SD. *$p < 0.05$, **$p < 0.01$, ***$p < 0.001$, ****$p < 0.0001$; ns, no significance.

expression is associated with poor prognosis.[22,23] Furthermore, the survivin DNA vaccine was found to delay tumor growth in a mouse model of PC.[24]

In this context, we hypothesized that OsFS vaccination, simultaneously remolding the TME and killing tumor cells, could be a novel immunotherapeutic for PC. Immunosuppressive Tregs and interleukin 10 (IL-10) may inhibit the anti-tumor immune responses induced by the vaccine.[25–27] Gemcitabine (Gem), a standard chemotherapeutic for advanced PC, has been shown to deplete Tregs *in vivo* without impairing the function of effector T cells.[28,29] In light of this evidence, we reasoned that Gem administration could further enhance the anti-tumor effect of the vaccine. Thus, we employed Panc02 murine PC models to explore the effects on tumor growth and survival of different OsFS/Gem combinations. Our results may provide the basis for the development of new effective therapies for PC.

RESULTS

Immunogenicity of OsFS in C57BL/6J mice

To investigate whether OsFS could stimulate cellular immune responses against murine FAPα and survivin in mice, we performed immunogenic experiments in healthy C57BL/6J mice (n = 5). Mice were immunized with vector control (Vec), OS, OsF, or OsFS three times with 2-week intervals. Two weeks after the third immunization, mice were euthanized, and splenocytes harvested for analysis. Splenocytes of vaccinated mice were stimulated with mixed FAPα, mixed survivin peptides (Figure S1), or unrelated peptides, and frequencies of antigen-specific interferon gamma (IFN-γ)-secreting T cells were measured by ELISpot assay. Compared with vector, OsFS could induce greater FAPα and survivin-specific T cell immune responses, the intensities of which did not notably differ from those of the single antigen vaccines (Figure 1A). However, OsFS induced both murine FAPα and survivin-specific cytotoxic T lymphocyte (CTL) responses in mice at three different effector:target (E:T) ratios (50:1, 25:1, 12.5:1), Moreover, the specific killing activity was significantly better than that of the OsF and OS groups when the E:T ratio was 50:1. (Figures 1B and 1C). The above results indicated that OsFS could stimulate cellular immune responses against murine FAPα and survivin in C57BL/6J mice and that mouse peptides could be used in subsequent experiments.

Anti-tumor activity of OsFS in a Panc02 murine PC model

We next evaluated the therapeutic efficacy of OsFS in an established Panc02 murine PC model. C57BL/6J mice (n = 5) were inoculated subcutaneously with 1×10^5 Panc02 cells and treated with Vec, Os, OsF, or OsFS on days 5, 7, and 10. Tumor growth was monitored for 20 days. As expected, all vaccines inhibit tumor growth. Moreover, OsFS could inhibit tumor growth substantially better than the single antigen vaccine (Figures 2A and 2B). The IFN-γ ELISpot assay revealed that, in Panc02-bearing mice, OsFS generated a higher number of FAPα and survivin-specific IFN-γ-releasing T cells compared with Vec. More importantly, there was no significant difference with single antigen vaccines (Figure 2C). Additionally, the relative proportions of immunoglobulin G2a (IgG2a) and IgG1 were also determined and showed that IgG2a was produced at significantly higher levels than IgG1. These results demonstrate that the vaccine tended to favor the development of T helper type 1 (Th1) over Th2 responses in C57BL/6J mice (Figure S2). The results demonstrated that OsFS could induce anti-Panc02 immune responses that inhibited tumor growth in an established Panc02 tumor model.

OsFS alters the TME

To further explore the impact of OsFS on the TME, we conducted quantitative real-time PCR analysis of mouse tumor tissues

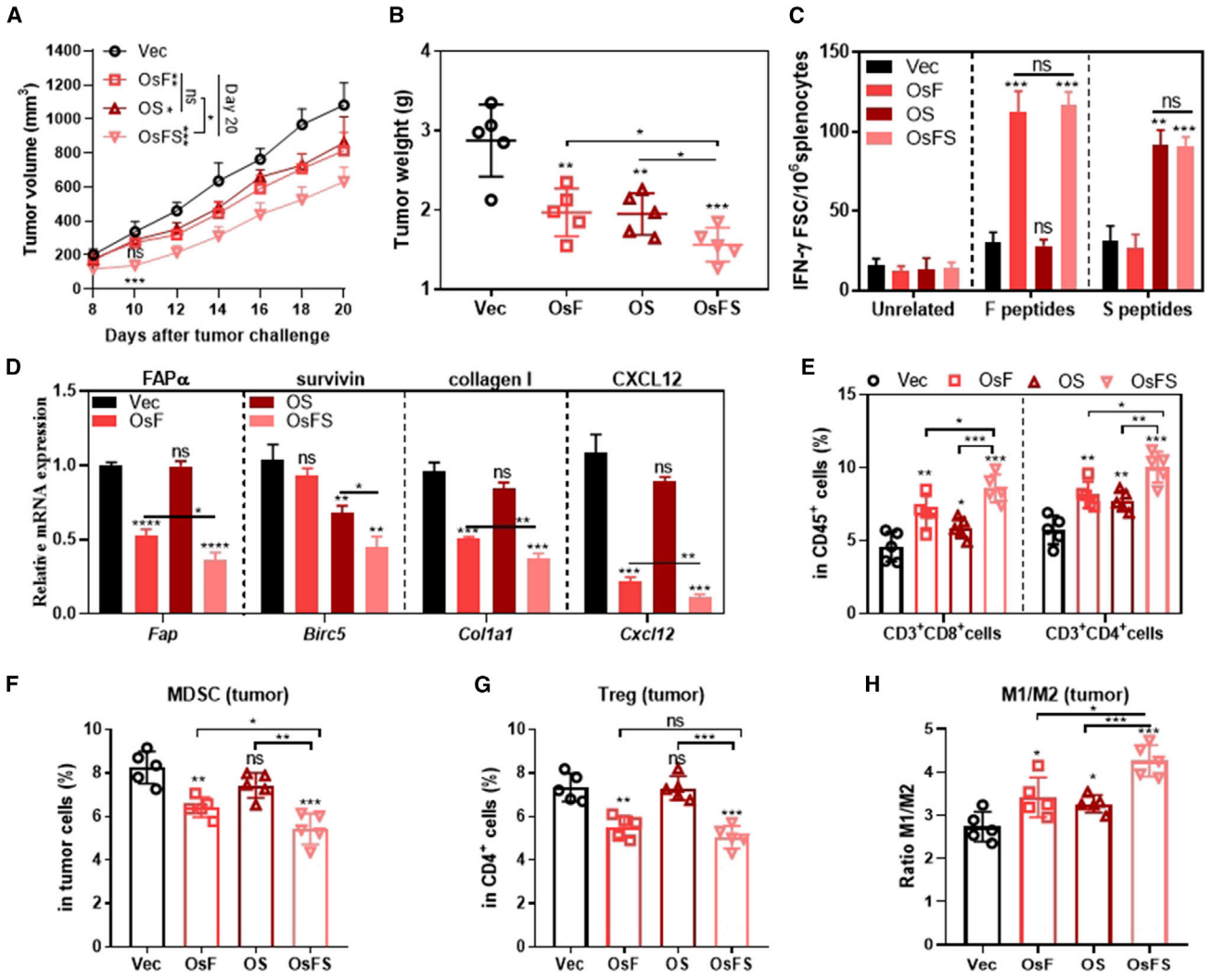

Figure 2. Therapeutic trials for anti-Panc02

(A) Tumor size was measured for 20 days after tumor inoculation (n = 5). (B) Mice were euthanized on day 20, tumors were isolated, and the tumor weights were measured. (C) ELISpot analysis of splenocytes after stimulation with FAPα- or survivin-specific peptides, with unrelated MUC1 peptides as a control. (D) Relative mRNA expression levels of FAPα, survivin (BRIC5), collagen I, and CXCL12 in tumors. GAPDH was used as an endogenous control. (E) The proportion of infiltrating $CD45^+$, $CD3^+CD8^+$, and $CD3^+CD4^+$ cells in tumors was measured by flow cytometry. (F–H) $CD11b^+Gr\text{-}1^+$ MDSCs (F) and the proportions of $CD4^+CD25^+Foxp3^+$ Tregs (in $CD4^+$ cells) (G) and TAMs ($CD11b^+F4/80^+CD206^-$ M1 and $CD11b^+F4/80^+CD206^+$ M2) (H) infiltrated into tumors. Statistical significance of differences between groups was determined by unpaired Student's t test. Error bars represent SD. *p < 0.05, **p < 0.01, ***p < 0.001, ****p < 0.0001; ns, no significance.

(Figure 2D). Our data suggested that, in Panc02-bearing mice, OsF could effectively reduce FAPα expression and OS reduce survivin expression, and OsFS significantly reduced tumor mRNA expression of both FAPα and survivin (Figures 2D and S3). In addition, OsF or OsFS treatment down-regulated the expression of *Col1a1* and *Cxcl12*, which are involved in tumor progression. However, the effect of OsFS was more significant than OsF, while OS did not have similar effect.

Our previous work suggested that OsFS could alter the TME by promoting tumor-infiltrating lymphocyte (TIL) infiltration and reducing the number of intratumoral CAFs in a murine breast cancer model.[21] Therefore, we reasoned that OsFS could exert similar effects on Panc02-derived tumors. As expected, OsFS or OsF not only promoted $CD3^+CD8^+$ and $CD3^+CD4^+$ T cell infiltration (Figure 2E) but also significantly reduced the proportion of $CD11b^+Gr\text{-}1^+$ MDSCs and $CD4^+CD25^+Foxp3^+$ Tregs in Panc02 tumors (Figures 2F and 2G) compared with the Vec. In addition, the ratio of intratumoral M1 ($CD11b^+F4/80^+CD86^+$) to M2 ($CD11b^+F4/80^+CD206^+$) macrophages was significantly higher than in the Vec group (Figure 2H), reflecting improved anti-tumor immunity. Obviously, OsFS was more effective compared with OsF. OS also induced more $CD3^+CD8^+$ T cells and $CD3^+CD4^+$ T cells compared with Vec. Although Tregs

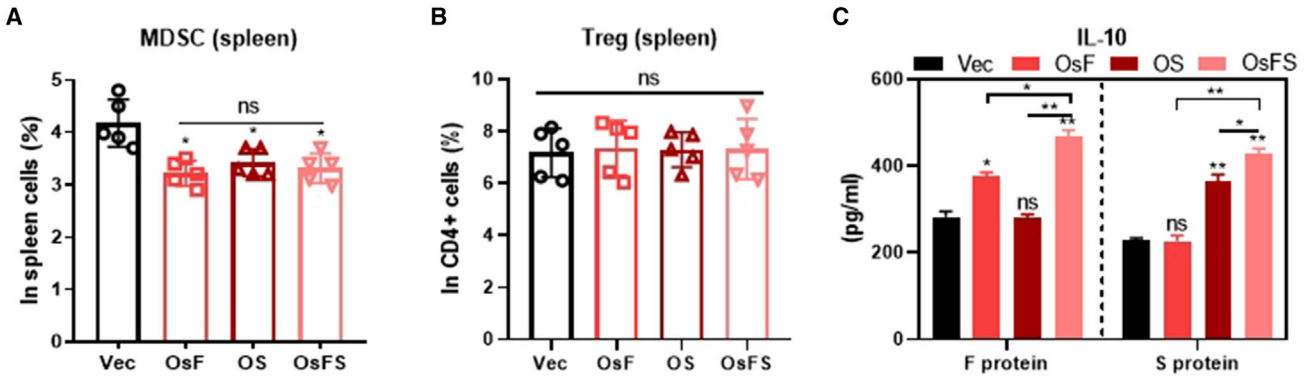

Figure 3. Detection of immunosuppressive factors

(A and B) The proportion of $CD11b^+Gr\text{-}1^+$ MDSCs (A) and $CD4^+CD25^+Foxp3^+$ Tregs (in $CD4^+$ cells) (B) in splenocytes. (C) The secretion of IL-10 from splenocytes following stimulation with FAPα or survivin for 3 days was measured by ELISA. Statistical significance of differences between groups was determined by unpaired Student's t test. Error bars represent SD. *$p < 0.05$, **$p < 0.01$; ns, no significance.

and MDSCs were not decreased, the ratio of M1 to M2 was increased (Figures 2E–2H). Taken together, these results clearly revealed that OsFS had a stronger ability to regulate the TME compared with single antigen vaccines OS or OsF.

The anti-tumor effects of OsFS are inhibited by regulatory cells

The DNA vaccine targeting FAPα is capable of reducing the tumor recruitment of MDSCs.[20] As expected, flow cytometry analysis showed that the proportion of MDSCs in the spleens of vaccine-treated mice was decreased compared with the controls (Figure 3A). We next examined the proportion of Tregs in the spleens of tumor-bearing mice. However, a substantial proportion of Tregs were still present in the spleen, which most likely resulted in the attenuation of the vaccine-induced immune responses (Figure 3B). Of note, after antigen stimulation, IL-10 secretion by splenocytes was 50% higher in the OsFS than in the Vec group (Figure 3C).

Altogether, these results indicated that although OsFS could reduce the proportion of immunosuppressive cells in Panc02 tumors, systemic Tregs and IL-10 were still capable of diminishing the anti-tumor response in vaccinated mice.

OsFS synergizes with Gem in inducing anti-tumor effects

Gem is a standard drug for the treatment of advanced PC and is able to selectively deplete Tregs and decreased IL-10 expression at low doses.[28] Thus, we hypothesized that the anti-tumor effects of OsFS could be enhanced by its combination with low-dose Gem (15 mg/kg).

To further clarify the anti-tumor mechanism of OsFS combined with Gem, we set up two combination groups (n = 5): combination I (Gem+OsFS I: Gem administration and vaccination simultaneously) and combination II (Gem+OsFS II: Gem administration after the final vaccination) (Figure 4A). As expected, both combination groups resulted in enhanced inhibition of tumor growth compared with the single treatments (Figures 4B and 4C). Interestingly, the anti-tumor effect of combination I was stronger than that of combination II. Specifically, the tumor inhibition rates were 84.4% and 62% after treatment with combinations I and II, respectively, compared with control mice (Figure 4C). The expression of antigens in combination-I-treated mice was significantly lower than in mice treated with OsFS (Figure 4D).

To evaluate the effect of combination therapies on mouse survival, the same five groups of mice (n = 10 per group) were treated as indicated in Figure 4A. Except for 30% of the mice treated with combination I, who were still alive on day 70, all other mice were dead by day 59 after Panc02 inoculation (Figure 4E). Mice treated with combinations I and II exhibited survival times 69.2% and 40.6% longer, respectively, compared with the untreated group.

Evaluation of immunomodulatory effect of gem

To gain further insights into the effect of Gem on anti-tumor immunity, MDSC, Treg and IL-10 were detected. Cytometry demonstrated that Gem had no effect on DMSC in spleen (Figure 5A), but it reduced the proportion of Tregs (Figure 5B). Further splenic expression of IL-10 was significantly decreased when OsFS and Gem were combined (Figure 5C). ELISpot analysis showed that Gem administration did not affect vaccine-induced, antigen-specific cellular immunity and further enhanced the ability to induce an immune response (Figure 5D). Moreover, flow cytometry analyses revealed that combination I was the most effective condition in promoting tumor infiltration of $CD3^+CD8^+$ and $CD3^+CD4^+$ T cells (Figure 5E). These results revealed that Gem administration could boost the anti-tumor effect of OsFS and that distinct treatment regimens could result in different efficacies.

Therapeutic effect of combination therapy in an orthotopic model of PC

To better mimic the human PC condition, a total of 1×10^6 Panc02 cells were injected into the pancreas of mice. Survival analyzes of Panc02-bearing mice treated with different therapies (n = 10). Since

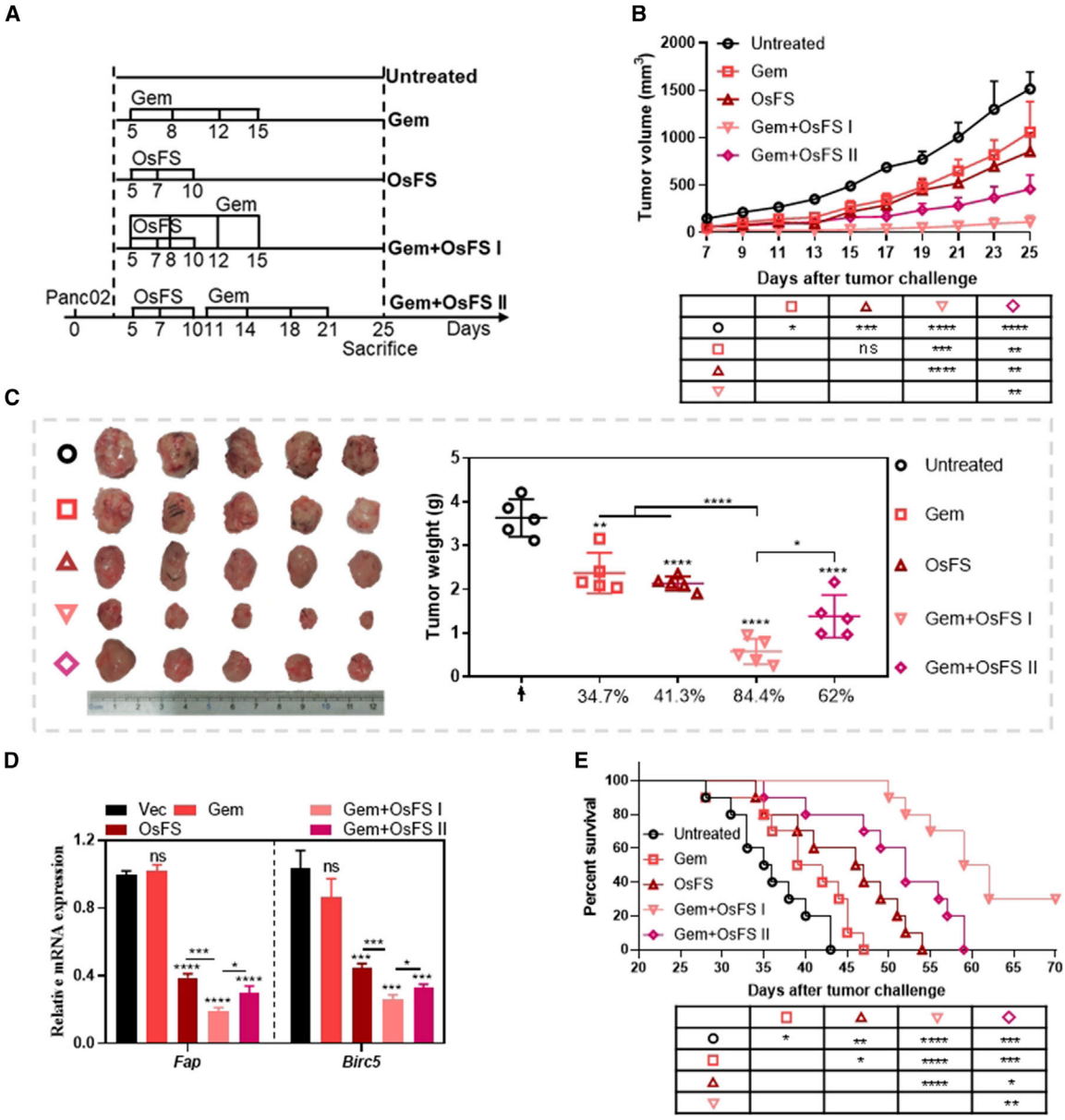

Figure 4. Effects of different combination therapies on tumor growth and anti-tumor immune response

(A) Experimental design of combination therapy, therapeutic strategies, and schedule (n = 5 mice per group). (B) Tumor volume was measured every 2 days following tumor challenge for 25 days. (C) Representative tumor (left) and tumor weight (right) upon harvest on day 25. (D) Relative mRNA expression levels of FAPα and survivin (BRIC5) in tumors. GAPDH was used as an endogenous control. (E) Survival analyses of Panc02-bearing mice treated with different combination therapies (n = 10). Statistical significance of differences between groups was determined by unpaired Student's t test. Error bars represent SD. *p < 0.05, **p < 0.01, ***p < 0.001, ****p < 0.0001; ns, no significance.

the therapeutic effect of combination I was superior to that of combination II, this experiment only evaluated the therapeutic effect of the optimal combination I. The treatment strategy and drug dosage were the same as those in the Panc02 subcutaneous tumor model. Consistent with the Panc02 subcutaneous model, the combined therapy had the strongest anti-tumor effect and significantly improved mouse survival, as shown by the 70% survival rate at 56 days, at which time all mice in other groups died (Figure 6A). The weight of tumor-bearing mice was measured every 2 days after orthotopic tumor inoculation, and none of the treatments affected the growth of mice (Figure 6B). These results indicated that the combination therapy had a strong anti-tumor effect in the orthotopic model of PC, but other immunomodulators may be needed to enhance the effect.

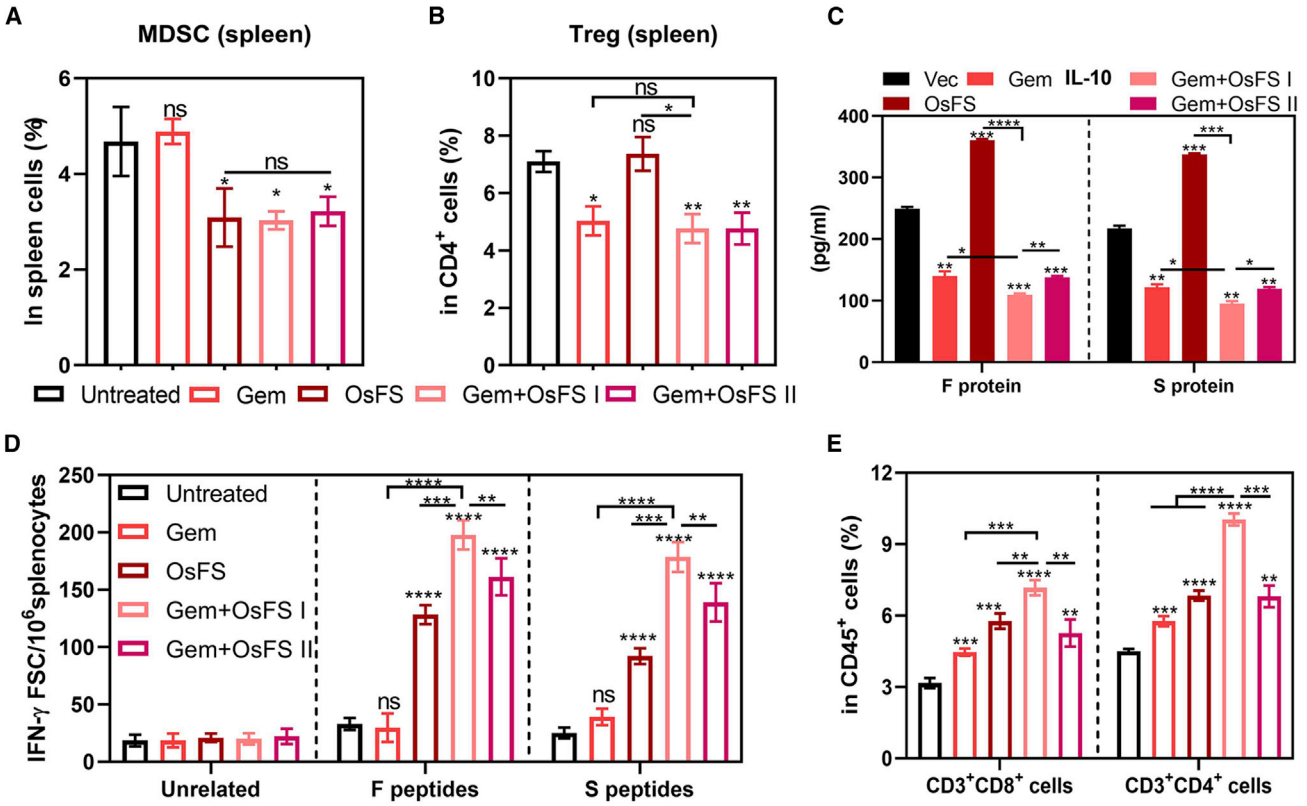

Figure 5. Explore the mechanism of combination therapy

(A and B) The proportions of $CD11b^+Gr\text{-}1^+$ MDSCs (A) and $CD4^+CD25^+Foxp3^+$ Tregs (in $CD4^+$ cells) (B) in spleen. (C) The secretion of IL-10 from splenocytes following stimulation with FAPα or survivin for 3 days was measured by ELISA. (D) ELISpot responses to mouse FAPα peptides and mouse survivin peptides, with unrelated hMUC1 peptides as a control. (E) The proportion of $CD3^+CD8^+$ and $CD3^+CD4^+$ cells in $CD45^+$ cells. Statistical significance of differences between groups was determined by unpaired Student's t test. Error bars represent SD. *$p < 0.05$, **$p < 0.01$, ***$p < 0.001$, ****$p < 0.0001$; ns, no significance.

DISCUSSION

As an important component of the immunosuppressive TME, CAFs have been proven to promote the progression and invasion of various solid tumors.[12,30–33] Nevertheless, the role of CAFs in the progression of PC is still debated.[4,14,34] Although some studies have demonstrated the CAF contribution to PC growth,[8,12] evidence in support of their inhibitory action on PC progression and invasion have also been reported.[16,17] These discrepancies may be due to the heterogeneity of the CAF population.[13–15] Cellular markers for CAFs include alpha-smooth muscle actin (αSMA), fibroblast-specific protein-1 (FSP-1), stromal cell-derived factor-1α (SDF-1α; CXCL12), and FAPα.[34] Indeed, depletion of αSMA^+ CAFs and some components of the tumor stroma in PC accelerates tumor growth and decreases survival.[16,17] Encouragingly, a previous study has shown that the depletion of FAP^+ CAFs in a mouse model of PC enhances the anti-tumor effect of immunotherapy and causes tumor regression.[18] This suggested that effective CAF-targeted treatments may require the combination of multiple therapeutic strategies, possibly including cancer vaccines and chemotherapeutics.

Therefore, to achieve optimal therapeutic effects, it may be necessary to target tumor cells while depleting $FAP\alpha^+$ CAFs, thus preventing ECM remodeling. OsFS meets both these requirements and, therefore, may be an effective vaccine for PC. In an established subcutaneous model based on Panc02-derived tumors, OsFS promoted T cell infiltration while significantly reducing the proportion of intratumoral $FAP\alpha^+$ CAFs, as well as antigen (FAPα and survivin) expression, leading to excellent inhibition of tumor growth. However, it is worth noting that since vaccine immunization followed tumor formation, immunosuppressive cells and cytokines preventing anti-tumor immunity had been most likely induced by the time of vaccination.[35,36] Hence, OsFS may have not reached its maximal efficacy in the established Panc02 tumor model.

Many studies have shown that immunosuppressive cells in tumor-bearing mice and patients with cancer may inhibit vaccine-induced anti-tumor effects. For example, 4T1 tumors induce a large number of systemic MDSCs.[21,37,38] We wondered whether Panc02 tumors could also promote MDSC production. In fact, no systemic MDSC surge was observed in the Panc02 tumor model, and OsFS treatment reduced the number of MDSCs in the spleen. However, another immunosuppressive cell type, Tregs, also contributing to the patient's poor prognosis,[25–27] caught our attention. The results showed that a

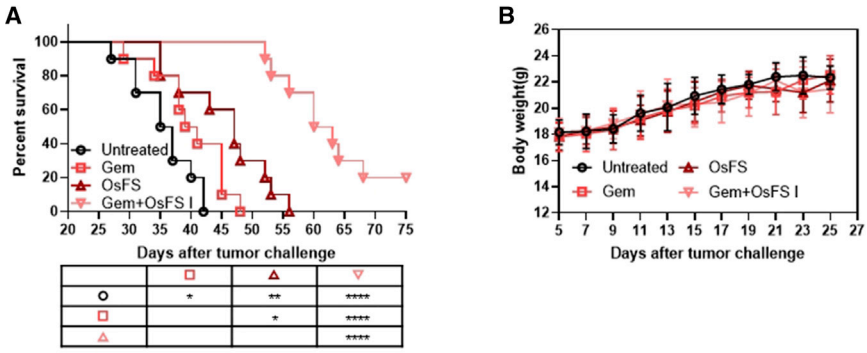

Figure 6. Combination I treatment showed significant survival benefit compared with single treatments in a Panc02 orthotopic injection model

(A) Survival analyses of Panc02-bearing mice treated with different combination therapies (n = 10). (B) The weight of tumor-bearing mice was measured every 2 days after subcutaneous tumor inoculation. Statistical significance of differences between groups was determined by unpaired Student's t test. Error bars represent SD. *p < 0.05, **p < 0.01, ****p < 0.0001.

relatively high proportion of Tregs were present in the spleen and that the expression of IL-10 was elevated in OsFS-treated tumor-bearing mice, which could interfere with the anti-tumor immune response induced by OsFS. Our results also indicated that the intensity and type of immunosuppressive effects might depend on the cancer type.

Several studies have demonstrated that low-dose chemotherapeutic drugs such as cyclophosphamide[25,26] and Gem[28,29] cause depletion of Tregs in tumor-bearing animals and patients with cancer. As an agent for the treatment of PC, Gem was shown to deplete Tregs without hampering the anti-tumor function of effector T cells.[28,29] Hence, we reasoned that the combination of low-dose Gem and OsFS could allow for optimal vaccine-induced anti-tumor immune responses. In line with this prediction, Gem enhanced OsFS-induced anti-tumor effects. Moreover, Gem administration resulted in enhanced Panc02-specific cellular immune responses. Both tested OsFS/Gem combination schedules resulted in increased proportion of TILs, while the number of immunosuppressive cells was further decreased compared with the single treatments. Of note, two alternative combination strategies, based on the same dose of Gem, resulted in different extents of tumor inhibition. In particular, the simultaneous administration of vaccine and Gem (combination I) was more effective compared with when Gem treatment was initiated a few days after vaccine inoculation (combination II). The reason for this could be that early Gem administration caused Treg depletion before vaccine-induced activation of immune responses, thus contributing to an ideal immune environment.

We further demonstrated that, in addition to inhibiting the growth of Panc02 tumors, the Gem/OsFS combination significantly prolonged the survival of tumor-bearing mice in an orthotopic Panc02 model. However, although the combination therapy resulted in improved anti-tumor effects compared with the single treatments, 80% of the tumor-bearing mice still died, indicating that additional factors were crucial for the therapeutic outcome. Flow cytometry analysis showed that many TILs were exhausted due to upregulation of PD-1(Figure S4). Therefore, PD-1 blocking strategies (e.g., PD-1 or PD-L1 monoclonal antibodies [mAbs]) might result in better anti-tumor effects.[39,40] This hypothesis needs to be experimentally verified.

Taken together, our results suggested that low-dose Gem administration significantly improved the anti-tumor effects of OsFS vaccination via the dual targeting of FAPα^+ CAFs and tumor cells. The described combination therapy may inspire the development of new approaches for the clinical management of PC.

MATERIALS AND METHODS

Cell lines

The murine PC cell line Panc02 was generously provided by Dr. Guang-Jun Nie (National Center for Nanoscience and Technology, Beijing, China), and was cultured in Dulbecco's modified Eagle's medium (DMEM) (Sigma Chemical, St. Louis, MO, USA) containing 10% fetal bovine serum (FBS) and was maintained at 37°C in a humidified incubator with 5% CO_2.

Animal model

Female C57BL/6J mice (6 to 8 weeks old) were purchased from Beijing Huafukang Biology Technology (Beijing, China) and raised in the animal experiment platform of College of Life Sciences, Jilin University. For subcutaneous tumor cell inoculation, 1×10^5 murine Panc02 PC cells were subcutaneously (s.c.) injected into the right lower flank of female C57BL/6J mice. Five days after tumor inoculation, the mice were randomized into different groups. Body weight and tumor volume of the tumor-bearing mice were measured every 2 days. Tumor volume = (length·width^2)/2(mm^3). For ethical reasons, tumor-bearing mice were euthanized when the tumor size was >2,000 mm^3. To establish the orthotopic mouse model of PC, mice were anesthetized by injection of 1% pentobarbital (70 mg/kg body weight, intraperitoneally [i.p.]), and an abdominal incision was performed under sterile conditions. A total of 1×10^6 Panc02 cells was injected into the pancreas. Peritoneum and skin were occluded using synthetic absorbable suture material. Five days after tumor inoculation, mice were randomized and divided into 4 groups for different treatments. Body weight was measured every 2 days until the mice began to die, and survival was monitored daily.

All animal experiments in this study were approved by the Ethics Committees of Jilin University.

Flow cytometry staining antibodies

The following antibodies were purchased from BioLegend (San Diego, CA, USA): anti-CD4-PE-CY7, anti-CD8-APC, anti-CD3-FITC, anti-CD45-PE, anti-Gr-1-APC, anti-CD11b-PE, anti-F4/80-FITC,

anti-CD206-APC, anti-CD86-PE-CY7, anti-CD4-FITC, anti-CD25-APC, anti-Foxp3-PE, anti-PD-1-FITC, anti-Tim3-PE-CY7, TruStain FcX PLUS (anti-mouse CD16/32), and isotype control. Antibody concentrations were used according to the manufacturer's instructions.

Epitope peptides prediction and synthesis

HLA-A*02:01 and HLA-A*24:02 are the most common HLA alleles, and HLA-A*02:01 was expressed in approximately 35% of patients.[41] The major histocompatibility complex (MHC) class I (HLA-A*02: 01, HLA-A*24: 02, H-2 Db, and H-2 Kb)-binding predictions for FAPα and survivin peptides were performed by the IEDB analysis resource Consensus tool (http://tools.iedb.org/main/tcell/),[42] which combines predictions from ANN, also known as NetMHC (4.0),[43–45] SMM,[46] and Comblib.[47] Selection criteria for FAPα peptides were as follows: MHC half maximal inhibitory concentration [IC_{50}] $\leq$ 500, total score ≥ -1; selection criteria for survivin peptides were as follows: MHC IC_{50} $\leq$5,000, total score ≥ -1.5. The sequence of the selected human and mouse peptides was identical or differed by 1–2 amino acids (Figure S1). All peptides were synthesized by Shanghai GL Peptide (Shanghai, China) at 95% purity.

Preparation of vaccines

The plasmids OsF, OS, and OsFS were previously constructed in our laboratory.[20] The plasmids were amplified in *Escherichia coli* DH5α cells and isolated by using a QIAGEN Plasmid Maxi Kit (Qigen, Germantown, MD, USA) to a purity >90% for supercoiled DNA and endotoxins <1 EU/mg.

In vivo tumor treatment strategies

In immunogenicity assays for the identification of antigenic epitope-associated peptides, female C57BL/6J mice (n = 5 per group) were immunized with the three plasmids (100 μg) or the Vec plasmid as a control via intramuscular (i.m.) injection into the tibialis anterior muscles of both hind limbs on days 0, 14, and 28. Two weeks after the last immunization, mice were euthanized for further evaluation. In a therapeutic setting, female C57BL/6J tumor-bearing mice (n = 5 per group) were immunized three times, on days 5, 7, and 10. The mice were euthanized on day 20. In the experiments with the vaccine/Gem combination, mice (n = 5 per group) were injected with Gem (15 mg/kg body weight, i.p.; Jiangsu Hansoh Pharmaceutical, Jiangsu, China) on days 5, 8, 12, and 15 (combination I: Gem + OsFS I) or on days 11, 14, 18, and 21 (combination II: Gem + OsFS II). The mice were euthanized on day 25. The first vaccination in all experiments was administrated i.m. by electroporation (TERESA, Shanghai, China), Electroporation parameters are pulse voltage 36 V, pulse width 20 ms, and pulse number 6. All mice were euthanized by exposure to carbon dioxide (CO_2).

IFN-γ ELISpot assay and *in vitro* cytotoxicity assay

The IFN-γ ELISpot assay was performed with ELISpot kit (BD Biosciences, San Jose, CA, USA), and *in vitro* cytotoxicity assays were conducted in accordance with previous studies.[48,49] In the antigen-specific ELISpot assay, mouse FAPα and survivin peptide pools (FAPα peptide pools: YVYQNNIYL, YSYTATYYI, HLYTHMTHF, FAVNWITYL, IYSERFMGL, and SSWEYYASI; survivin peptide pools: ATFKNWPFL, IATFKNWPF, QCFFCFKEL, and LTVSEFLKL) were chosen as the stimulators, with the unrelated MUC1 peptide pool (GVTSAPDTR, SAPDTRPAP, DTRPAPGST, PAPGSTAPP, and TRPAPGSTA) as the control. To detect antigen-specific CTLs, Panc02 cells were incubated with FAPα, survivin, or an unrelated MUC1 peptide (5 μg/mL) for 2 h at 37°C. Then, FAPα or survivin-peptide-loaded Panc02 cells were labeled with 5 μM CFSE (CFSE-high cells) for 10 min, while the unrelated-MUC1-peptide-loaded Panc02 cells were labeled only with 0.5 μM CFSE (CFSE-low cells). CFSE-high- and -low-labeled cells were mixed together at a 1:1 ratio. Different numbers of splenocytes from vaccinated mice were then incubated with 5×10^4 of the peptide-loaded Panc02 cells for 8 h at 37 C (E:T ratios were 50:1, 25:1, and 12.5). Specific killing was detected by flow cytometry as the decrease in the percentage of specific targets.

RNA isolation and quantitative real-time PCR

RNA isolation used Trizol (Invitrogen, Carlsbad, CA, USA), and the cDNA was synthesized with a PrimeScript RT Reagent Kit with Genomic DNA (gDNA) Eraser (TaKaRa, Shiga, Japan), in accordance with the manufacturer's instructions. Quantitative real-time PCR was performed as previously described.[50] Gene-expression levels were normalized to *Gapdh* expression.

Ig isotyping by ELISA

Serum IgG1 and IgG2a were measured using the mouse immunoglobulin screening/isotyping kit (Southern Biotech). 96-well flat-bottom microplates were coated with FAPα or survivin recombinant proteins (0.2 μg/well) overnight at 4°C. Sera collected from mice prior to sacrifice were diluted 1:25 in PBS with 1% FBS before detection. The remaining steps of the procedure were performed as previously described.[50]

IL-10 detection by ELISA

IL-10 was measured using a mouse Il-10 ELISA MAX Standard (Biolegend, San Diego, CA, USA). 1×10^7 splenocytes were resuspended in 500 μL RPMI 1640 supplemented with 10% FBS, stimulated with FAPα or survivin protein (5 μg/mL), for 3 days in 12-well plates. Cell culture supernatants of the stimulated splenocytes were diluted 1:3 in PBS with 1% FBS before detection. The remaining steps were conducted according to manufacturer's instructions.

Cell staining and flow cytometry

For detection of $CD45^+$, $CD3^+$, $CD4^+$, $CD8^+$ T, MDSCs ($CD11b^+$ $Gr\text{-}1^+$), M1 macrophages ($CD11b^+F4/80^+CD86^+$), and M2 macrophages ($CD11b^+F4/80^+CD206^+$), separated splenocytes or tumor cells were washed twice with PBS and stained with fluorescently labeled antibodies for 25–30 min at 4°C.

For detection of intratumoral $FAP\alpha^+$ CAFs, after washing, tumor cells were immunostained with a rabbit anti-FAPα antibody (Abcam, Cambridge, UK) or normal rabbit IgG control antibody at 4°C for 60 min. Cells were then stained with sheep anti-rabbit FITC

secondary antibody (Biolegend, San Diego, CA, USA) for at least 30 min at 4°C.

After washing twice, all samples (resuspended with 350 μL of cell staining buffer; Biolegend, San Diego, CA, USA) were examined by a BD Accuri C6 flow cytometer (BD Biosciences, San Jose, CA USA), and data were analyzed using FlowJo software (TreeStar, San Carlos, CA, USA).

Intracellular cytokine staining

To detect Tregs ($CD4^+CD25^+Foxp3^+$), separated cells were incubated with surface stain for 25–30 min at 4°C, and intracellular cytokine staining was performed using the Foxp3/Transcription Factor Staining Buffer Set (eBioscience). The cells were then fixed and permeabilized for 1 h at room temperature. After incubation with anti-mouse CD16/32 (Fc block) antibody for 15 min, cells were incubated in intracellular stain (anti-$Foxp3^+$) for at least 60 min at room temperature. After washing, samples were analyzed by flow cytometry.

Statistical analysis

All statistical analyses were performed using GraphPad Prism 8.0 (La Jolla, CA, USA). Data were analyzed using one-way ANOVA and are presented as mean ± SD. The statistical significance of differences between groups was determined by unpaired Student's t test. The statistical analysis of survival data was performed using log rank test. $p < 0.05$ was considered statistically significant.

Data availability statement

All relevant data of this study are available from the corresponding author upon request.

SUPPLEMENTAL INFORMATION

Supplemental information can be found online at https://doi.org/10.1016/j.omto.2022.07.008.

ACKNOWLEDGMENTS

We thank Dr. Guang-Jun Nie from the National Center for Nanoscience and Technology, Beijing, China, for providing the Panc02 cancer cell line. This research was supported by the Key R & D Projects of Science and Technology Department of Jilin Province (grant no. 20180201001YY), Major Projects of Science and Technology Innovation in Changchun City (grant no. 17YJ002), the Specialized Research Fund for the National Natural Science Foundation of China (grant no. 31300765), the Jilin Province Science and Technology Development Program (grant no. 20160519018JH), and the National Science and Technology Major Project of the Ministry of Science and Technology of China (grant no. 2014ZX09304314-001).

AUTHOR CONTRIBUTIONS

H.Z., X.Y., B.Y., H.W., J.W. and W.K. designed and supervised the study. F.G., L.D., X.B., Q.G., J.G., and Y.Z. conducted the experiments. F.G. and L.D. wrote the paper.

DECLARATION OF INTERESTS

The authors declare no conflicts of interest.

REFERENCES

1. Siegel, R.L., Miller, K.D., Fuchs, H.E., and Jemal, A. (2021). Cancer statistics, 2021. CA. Cancer J. Clin. *71*, 7–33. https://doi.org/10.3322/caac.21654.
2. Ryan, D.P., Hong, T.S., and Bardeesy, N. (2014). Pancreatic adenocarcinoma. N. Engl. J. Med. *371*, 1039–1049. https://doi.org/10.1056/NEJMra1404198.
3. Zhou, B., Xu, J.W., Cheng, Y.G., Gao, J.Y., Hu, S.Y., Wang, L., and Zhan, H.X. (2017). Early detection of pancreatic cancer: where are we now and where are we going? Int. J. Cancer *141*, 231–241. https://doi.org/10.1002/ijc.30670.
4. Karamitopoulou, E. (2019). Tumour microenvironment of pancreatic cancer: immune landscape is dictated by molecular and histopathological features. Br. J. Cancer *121*, 5–14. https://doi.org/10.1038/s41416-019-0479-5.
5. Sun, Q., Zhang, B., Hu, Q., Qin, Y., Xu, W., Liu, W., Yu, X., and Xu, J. (2018). The impact of cancer-associated fibroblasts on major hallmarks of pancreatic cancer. Theranostics *8*, 5072–5087. https://doi.org/10.7150/thno.26546.
6. Kalluri, R. (2016). The biology and function of fibroblasts in cancer. Nat. Rev. Cancer *16*, 582–598. https://doi.org/10.1038/nrc.2016.73.
7. Weniger, M., Honselmann, K.C., and Liss, A.S. (2018). The extracellular matrix and pancreatic cancer: a complex relationship. Cancers (Basel) *10*, E316. https://doi.org/10.3390/cancers10090316.
8. Wei, L., Ye, H., Li, G., Lu, Y., Zhou, Q., Zheng, S., Lin, Q., Liu, Y., Li, Z., and Chen, R. (2018). Cancer-associated fibroblasts promote progression and gemcitabine resistance via the SDF-1/SATB-1 pathway in pancreatic cancer. Cell Death Dis. *9*, 1065. https://doi.org/10.1038/s41419-018-1104-x.
9. Kudo-Saito, C., Shirako, H., Ohike, M., Tsukamoto, N., and Kawakami, Y. (2013). CCL2 is critical for immunosuppression to promote cancer metastasis. Clin. Exp. Metastasis *30*, 393–405. https://doi.org/10.1007/s10585-012-9545-6.
10. Feig, C., Jones, J.O., Kraman, M., Wells, R.J.B., Deonarine, A., Chan, D.S., Connell, C.M., Roberts, E.W., Zhao, Q., Caballero, O.L., et al. (2013). Targeting CXCL12 from FAP-expressing carcinoma-associated fibroblasts synergizes with anti-PD-L1 immunotherapy in pancreatic cancer. Proc. Natl. Acad. Sci. USA *110*, 20212–20217. https://doi.org/10.1073/pnas.1320318110.
11. Zhang, Y., Crawford, H.C., and Pasca di Magliano, M. (2019). Epithelial-stromal interactions in pancreatic cancer. Annu. Rev. Physiol. *81*, 211–233. https://doi.org/10.1146/annurev-physiol-020518-114515.
12. Shan, T., Chen, S., Chen, X., Lin, W.R., Li, W., Ma, J., Wu, T., Cui, X., Ji, H., Li, Y., and Kang, Y. (2017). Cancer-associated fibroblasts enhance pancreatic cancer cell invasion by remodeling the metabolic conversion mechanism. Oncol. Rep. *37*, 1971–1979. https://doi.org/10.3892/or.2017.5479.
13. Öhlund, D., Handly-Santana, A., Biffi, G., Elyada, E., Almeida, A.S., Ponz-Sarvise, M., Corbo, V., Oni, T.E., Hearn, S.A., Lee, E.J., et al. (2017). Distinct populations of inflammatory fibroblasts and myofibroblasts in pancreatic cancer. J. Exp. Med. *214*, 579–596. https://doi.org/10.1084/jem.20162024.
14. Bijlsma, M.F., and van Laarhoven, H.W.M. (2015). The conflicting roles of tumor stroma in pancreatic cancer and their contribution to the failure of clinical trials: a systematic review and critical appraisal. Cancer Metastasis Rev. *34*, 97–114. https://doi.org/10.1007/s10555-014-9541-1.
15. Ligorio, M., Sil, S., Malagon-Lopez, J., Nieman, L.T., Misale, S., Di Pilato, M., Ebright, R.Y., Karabacak, M.N., Kulkarni, A.S., Liu, A., et al. (2019). Stromal microenvironment shapes the intratumoral architecture of pancreatic cancer. Cell *178*, 160–175.e27. https://doi.org/10.1016/j.cell.2019.05.012.
16. Rhim, A.D., Oberstein, P.E., Thomas, D.H., Mirek, E.T., Palermo, C.F., Sastra, S.A., Dekleva, E.N., Saunders, T., Becerra, C.P., Tattersall, I.W., et al. (2014). Stromal elements act to restrain, rather than support, pancreatic ductal adenocarcinoma. Cancer Cell *25*, 735–747. https://doi.org/10.1016/j.ccr.2014.04.021.
17. Özdemir, B.C., Pentcheva-Hoang, T., Carstens, J.L., Zheng, X., Wu, C.C., Simpson, T.R., Laklai, H., Sugimoto, H., Kahlert, C., Novitskiy, S.V., et al. (2014). Depletion of carcinoma-associated fibroblasts and fibrosis induces immunosuppression and accelerates pancreas cancer with reduced survival. Cancer Cell *25*, 719–734. https://doi.org/10.1016/j.ccr.2014.04.005.

18. Kraman, M., Bambrough, P.J., Arnold, J.N., Roberts, E.W., Magiera, L., Jones, J.O., Gopinathan, A., Tuveson, D.A., and Fearon, D.T. (2010). Suppression of antitumor immunity by stromal cells expressing fibroblast activation protein-alpha. Science *330*, 827–830. https://doi.org/10.1126/science.1195300.

19. Lee, H.O., Mullins, S.R., Franco-Barraza, J., Valianou, M., Cukierman, E., and Cheng, J.D. (2011). FAP-overexpressing fibroblasts produce an extracellular matrix that enhances invasive velocity and directionality of pancreatic cancer cells. BMC Cancer *11*, 245. https://doi.org/10.1186/1471-2407-11-245.

20. Geng, F., Guo, J., Guo, Q.Q., Xie, Y., Dong, L., Zhou, Y., Liu, C.L., Yu, B., Wu, H., Wu, J.X., et al. (2019). A DNA vaccine expressing an optimized secreted FAPalpha induces enhanced anti-tumor activity by altering the tumor microenvironment in a murine model of breast cancer. Vaccine *37*, 4382–4391. https://doi.org/10.1016/j.vaccine.2019.06.012.

21. Geng, F., Bao, X., Dong, L., Guo, Q.Q., Guo, J., Xie, Y., Zhou, Y., Yu, B., Wu, H., Wu, J.X., et al. (2020). Doxorubicin pretreatment enhances FAPalpha/survivin co-targeting DNA vaccine anti-tumor activity primarily through decreasing peripheral MDSCs in the 4T1 murine breast cancer model. Oncoimmunology *9*, 1747350. https://doi.org/10.1080/2162402X.2020.1747350.

22. Kami, K., Doi, R., Koizumi, M., Toyoda, E., Mori, T., Ito, D., Fujimoto, K., Wada, M., Miyatake, S.I., and Imamura, M. (2004). Survivin expression is a prognostic marker in pancreatic cancer patients. Surgery *136*, 443–448. https://doi.org/10.1016/j.surg.2004.05.023.

23. Yang, X.P., Liu, S.L., Xu, J.F., Cao, S.G., Li, Y., and Zhou, Y.B. (2017). Pancreatic stellate cells increase pancreatic cancer cells invasion through the hepatocyte growth factor/c-Met/survivin regulated by P53/P21. Exp. Cell Res. *357*, 79–87. https://doi.org/10.1016/j.yexcr.2017.04.027.

24. Zhu, K., Qin, H., Cha, S.C., Neelapu, S.S., Overwijk, W., Lizee, G.A., Abbruzzese, J.L., Hwu, P., Radvanyi, L., Kwak, L.W., and Chang, D.Z. (2007). Survivin DNA vaccine generated specific antitumor effects in pancreatic carcinoma and lymphoma mouse models. Vaccine *25*, 7955–7961. https://doi.org/10.1016/j.vaccine.2007.08.050.

25. Yamamoto, T., Yanagimoto, H., Satoi, S., Toyokawa, H., Hirooka, S., Yamaki, S., Yui, R., Yamao, J., Kim, S., and Kwon, A.H. (2012). Circulating CD4+CD25+ regulatory T cells in patients with pancreatic cancer. Pancreas *41*, 409–415. https://doi.org/10.1097/MPA.0b013e3182373a66.

26. Cappello, P., Curcio, C., Mandili, G., Roux, C., Bulfamante, S., and Novelli, F. (2018). Next generation immunotherapy for pancreatic cancer: DNA vaccination is seeking new combo partners. Cancers (Basel) *10*, E51. https://doi.org/10.3390/cancers10020051.

27. Takeuchi, Y., and Nishikawa, H. (2016). Roles of regulatory T cells in cancer immunity. Int. Immunol. *28*, 401–409. https://doi.org/10.1093/intimm/dxw025.

28. Shevchenko, I., Karakhanova, S., Soltek, S., Link, J., Bayry, J., Werner, J., Umansky, V., and Bazhin, A.V. (2013). Low-dose gemcitabine depletes regulatory T cells and improves survival in the orthotopic Panc02 model of pancreatic cancer. Int. J. Cancer *133*, 98–107. https://doi.org/10.1002/ijc.27990.

29. Eriksson, E., Wenthe, J., Irenaeus, S., Loskog, A., and Ullenhag, G. (2016). Gemcitabine reduces MDSCs, tregs and TGFbeta-1 while restoring the teff/treg ratio in patients with pancreatic cancer. J. Transl. Med. *14*, 282. https://doi.org/10.1186/s12967-016-1037-z.

30. Sandberg, T.P., Stuart, M.P.M.E., Oosting, J., Tollenaar, R.A.E.M., Sier, C.F.M., and Mesker, W.E. (2019). Increased expression of cancer-associated fibroblast markers at the invasive front and its association with tumor-stroma ratio in colorectal cancer. BMC Cancer *19*, 284. https://doi.org/10.1186/s12885-019-5462-2.

31. Jang, I., and Beningo, K.A. (2019). Integrins, CAFs and mechanical forces in the progression of cancer. Cancers (Basel) *11*, E721. https://doi.org/10.3390/cancers11050721.

32. Farhood, B., Najafi, M., and Mortezaee, K. (2019). Cancer-associated fibroblasts: secretions, interactions, and therapy. J. Cell. Biochem. *120*, 2791–2800. https://doi.org/10.1002/jcb.27703.

33. Shiga, K., Hara, M., Nagasaki, T., Sato, T., Takahashi, H., and Takeyama, H. (2015). Cancer-associated fibroblasts: their characteristics and their roles in tumor growth. Cancers (Basel) *7*, 2443–2458. https://doi.org/10.3390/cancers7040902.

34. von Ahrens, D., Bhagat, T.D., Nagrath, D., Maitra, A., and Verma, A. (2017). The role of stromal cancer-associated fibroblasts in pancreatic cancer. J. Hematol. Oncol. *10*, 76. https://doi.org/10.1186/s13045-017-0448-5.

35. Melief, C.J.M., van Hall, T., Arens, R., Ossendorp, F., and van der Burg, S.H. (2015). Therapeutic cancer vaccines. J. Clin. Invest. *125*, 3401–3412. https://doi.org/10.1172/JCI80009.

36. Finn, O.J. (2018). The dawn of vaccines for cancer prevention. Nat. Rev. Immunol. *18*, 183–194. https://doi.org/10.1038/nri.2017.140.

37. Hamilton, M.J., Banáth, J.P., Lam, V., Lepard, N.E., Krystal, G., and Bennewith, K.L. (2012). Serum inhibits the immunosuppressive function of myeloid-derived suppressor cells isolated from 4T1 tumor-bearing mice. Cancer Immunol. Immunother. *61*, 643–654. https://doi.org/10.1007/s00262-011-1125-0.

38. Younos, I.H., Dafferner, A.J., Gulen, D., Britton, H.C., and Talmadge, J.E. (2012). Tumor regulation of myeloid-derived suppressor cell proliferation and trafficking. Int. Immunopharmacol. *13*, 245–256. https://doi.org/10.1016/j.intimp.2012.05.002.

39. Balar, A.V., and Weber, J.S. (2017). PD-1 and PD-L1 antibodies in cancer: current status and future directions. Cancer Immunol. Immunother. *66*, 551–564. https://doi.org/10.1007/s00262-017-1954-6.

40. Du, W., Yang, M., Turner, A., Xu, C., Ferris, R.L., Huang, J., Kane, L.P., and Lu, B. (2017). TIM-3 as a target for cancer immunotherapy and mechanisms of action. Int. J. Mol. Sci. *18*, E645. https://doi.org/10.3390/ijms18030645.

41. Da Silva, D.M., Enserro, D.M., Mayadev, J.S., Skeate, J.G., Matsuo, K., Pham, H.Q., Lankes, H.A., Moxley, K.M., Ghamande, S.A., Lin, Y.G., et al. (2020). Immune activation in patients with locally advanced cervical cancer treated with ipilimumab following definitive chemoradiation (GOG-9929). Clin. Cancer Res. *26*, 5621–5630. https://doi.org/10.1158/1078-0432.CCR-20-0776.

42. Kim, Y., Ponomarenko, J., Zhu, Z., Tamang, D., Wang, P., Greenbaum, J., Lundegaard, C., Sette, A., Lund, O., Bourne, P.E., et al. (2012). Immune epitope database analysis resource. Nucleic Acids Res. *40*, W525–W530. https://doi.org/10.1093/nar/gks438.

43. Nielsen, M., Lundegaard, C., Worning, P., Lauemøller, S.L., Lamberth, K., Buus, S., Brunak, S., and Lund, O. (2003). Reliable prediction of T-cell epitopes using neural networks with novel sequence representations. Protein Sci. *12*, 1007–1017. https://doi.org/10.1110/ps.0239403.

44. Lundegaard, C., Lamberth, K., Harndahl, M., Buus, S., Lund, O., and Nielsen, M. (2008). NetMHC-3.0: accurate web accessible predictions of human, mouse and monkey MHC class I affinities for peptides of length 8-11. Nucleic Acids Res. *36*, W509–W512. https://doi.org/10.1093/nar/gkn202.

45. Andreatta, M., and Nielsen, M. (2016). Gapped sequence alignment using artificial neural networks: application to the MHC class I system. Bioinformatics *32*, 511–517. https://doi.org/10.1093/bioinformatics/btv639.

46. Peters, B., and Sette, A. (2005). Generating quantitative models describing the sequence specificity of biological processes with the stabilized matrix method. BMC Bioinfo. *6*, 132. https://doi.org/10.1186/1471-2105-6-132.

47. Sidney, J., Assarsson, E., Moore, C., Ngo, S., Pinilla, C., Sette, A., and Peters, B. (2008). Quantitative peptide binding motifs for 19 human and mouse MHC class I molecules derived using positional scanning combinatorial peptide libraries. Immunome Res. *4*, 2. https://doi.org/10.1186/1745-7580-4-2.

48. Xia, Q., Geng, F., Zhang, F.F., Liu, C.L., Xu, P., Lu, Z.Z., Zhang, H.H., Kong, W., and Yu, X.H. (2016). Enhancement of fibroblast activation protein alpha-based vaccines and adenovirus boost immunity by cyclophosphamide through inhibiting IL-10 expression in 4T1 tumor bearing mice. Vaccine *34*, 4526–4535. https://doi.org/10.1016/j.vaccine.2016.07.054.

49. Zhang, H., Wang, Y., Liu, C., Zhang, L., Xia, Q., Zhang, Y., Wu, J., Jiang, C., Chen, Y., Wu, Y., et al. (2012). DNA and adenovirus tumor vaccine expressing truncated survivin generates specific immune responses and anti-tumor effects in a murine melanoma model. Cancer Immunol. Immunother. *61*, 1857–1867. https://doi.org/10.1007/s00262-012-1296-3.

50. Wang, Y.Q., Zhang, H.H., Liu, C.L., Wu, H., Wang, P., Xia, Q., Zhang, L.X., Li, B., Wu, J.X., Yu, B., et al. (2013). Enhancement of survivin-specific anti-tumor immunity by adenovirus prime protein-boost immunity strategy with DDA/MPL adjuvant in a murine melanoma model. Int. Immunopharmacol. *17*, 9–17. https://doi.org/10.1016/j.intimp.2013.04.015.